VERSITA
DOI 10.2478/ama-2013-0033

DYNAMIC TESTING OF COPPER MATERIAL – NUMERICAL APPROACH

Paweł BARANOWSKI*, Jerzy MAŁACHOWSKI*, Łukasz MAZURKIEWICZ*, Krzysztof DAMAZIAK*

*Faculty of Mechanical Engineering, Department of Mechanics and Applied Computer Science, Military University of Technology, ul. Gen. Kaliskiego 2, 00-908 Warszawa, Poland

pbaranowski@wat.edu.pl, jerzy.malachowski@wat.edu.pl, lmazurkiewicz@wat.edu.pl, kdamaziak@wat.edu.pl

Abstract: Split Hopkinson pressure bar (SHPB) is one of the most important and recognisable apparatus used for characterizing the dynamic behaviour of various materials. Incident pulse generated one the incident bar usually have a rectangular shape, which is proper for some materials but for others is not. Therefore, several methods of shaping the incident pulse are used for obtaining constant strain rate conditions during tests. Very often pulse shapers made of copper or similar material are implemented due to its softness properties. In this paper such material was investigated using the FE model of SHPB. Its mechanical behaviour was characterised with and without copper disc between the striker and incident bar. Numerical simulations were carried out using explicit LS-DYNA code. Two different methods were used for modelling the copper sample: typical finite Lagrangian elements and meshless Smoothed Particle Hydrodynamics (SPH) method. As a result of two techniques used axial stress-strain characteristics were compared for three different striker's velocity with an influence of the copper pulse shaper taking into account. Finally, FE and SPH method was compared with taking into consideration: the efficiency, computer memory and power requirements, complexity of methods and time of simulation.

Key words: Copper, Compression, FE Analysis, SHPB

1. INTRODUCTION

Hopkinson bar with all its former and actual configurations is widely used to determine material properties at high strain rates (Ellwood et al., 1982; Hopkins, 1872). Such investigations, however, are exposed to longitudinal dispersion produced from indirect effects such as lateral impact of the striker. Also, Pochhammer-Chree oscillations (Davies, 1948; Graff, 2004) can occur, which affect the mechanical behaviour of tested sample. Therefore, several methods of shaping the pulse on the incident bar are used, e.g.: by inserting a preloading bar ((Ellwood et al., 1982;Foley et al., 2010; Franz et al., 1984) or using a pulse shaper (Ellwood et al., 1982; Foley et al., 2010; Naghdabadia et al., 2012), which very often is made of copper or similar material (due to its softness properties). In addition to the previous methods a shape of the striker is modified (Cloete et al., 2008; Li et al., 2005; Seng, 2003), which in fact was the investigation object of the previous authors' paper (Baranowski et al., 2013).

It is well known that for different test conditions it is recommended to adjust thickness and diameter of the pulse shaper (Foley et al., 2010). Also, work-hardening or brittle materials need different thickness-length proportion of the disc. Moreover, as presented by other authors (Klepaczko, 2007; Jankowiak et al., 2011), such effect like friction, apart from others, influences the proper estimation of material properties using SHPB, due to the overstress state in the specimen. Authors are aware of such foundations but the main purpose of the paper is to present the possibility of two different numerical techniques for characterising a mechanical behaviour of material with and without copper disc between the striker and incident bar. In experimental conditions the use of the pulse shaper is a simple procedure, but for obtaining a constant strain rate conditions during tests many attempts have to be conducted. This can be easily achieved using numerical methods, more particularly finite element method. Also, initial tests for calibrating the actual SHPB set-up can be performed, even using literature material properties.

In the paper numerical simulations were carried out using explicit LS-DYNA code. Two different methods were used for modelling the copper sample: typical finite Lagrangian elements and meshless Smoothed Particle Hydrodynamics (SPH) method, which is considered by authors as novel in terms of SHPB pulse shaper modelling. Subsequently, mechanical characteristics of the material (stress vs. strain curves) were compared for both methods and, additionally, for three different striker's velocities with an influence of the copper pulse shaper taking into account. Finally, FE and SPH method was compared with taking into consideration: the efficiency, computer memory and power requirements, complexity of methods and time of simulation.

Presented study is the part of wider investigations which are pointed on finding the optimal shape of incident pulse for a specific type of material (brittle, ductile or soft). In these studies copper material plays a major role (is used for the pulse disc), therefore our attention is also focused on the proper material constitutive material modelling.

2. SHPB TESTING – OPERATING PRINCIPLE

A typical SHPB test starts with launching a striker using highly compressed gas , which consequently impacts the incident bar. This generates the elastic wave (incident wave) which travels through the bar and then, due to the difference between mechanical impedances of bar and specimen materials, part of the pulse comes back (reflected wave), whereas the rest of it is transmitted through the tested specimen. Next, the specimen is compressed and the wave travels to the transmission bar and generates a so called transmitted wave (Fig. 1).

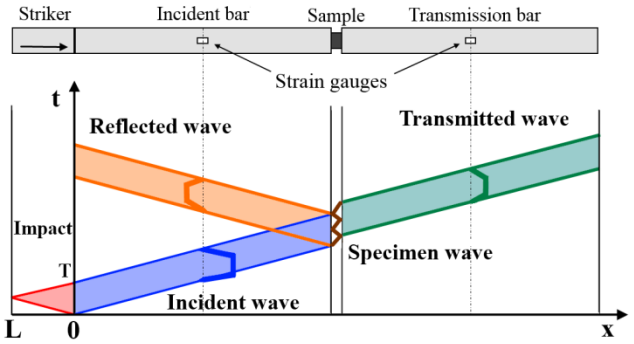

Fig. 1. Wave history route in SHPB

Based on the above Figure, in addition to the literature (Ellwood et al., 1982; Hopkins, 1872; Davies, 1948), it can be stated that pulse duration time increases proportionally with striker's length:

$$T = \frac{2L}{c_p} \tag{1}$$

where: T – impulse duration time, L – striker length and c_p – elastic wave propagation velocity in a bar material

All three signals are sensed by strain gauges which are placed in the middle of the bars. Then the relationship between three pulses (transmitted ε_T, incident ε_I and reflected ε_R) can be described as follows [1,2,5]:

$$\varepsilon_T(t) = \varepsilon_I(t) - \varepsilon_R(t) \tag{2}$$

According to the conventional one-dimensional SHPB theory, the nominal strain rate, strain and nominal stress in the specimen are given by Ellwood et al. (1982); Hopkins (1872) and Foley et al. (2010):

$$\dot{\varepsilon}(t) = -2\frac{C_0}{L_S}\varepsilon_R(t) \tag{3}$$

$$\varepsilon(t) = -2\frac{C_0}{L_S}\int_o^t \varepsilon_R(t)dt \tag{4}$$

$$\sigma(t) = -\frac{ES_{p0}}{S_{pr}}\varepsilon_T(t) \tag{5}$$

where C_o – wave velocity in incident bar, L_s – specimen length, E – Young modulus, S_{po} – cross section area of transmitted bar, S_{pr} – cross section area of specimen, $\varepsilon_R(t)$ – reflected strain history, $\varepsilon_T(t)$ – transmitted strain history.

3. NUMERICAL SHPB TESTING

The FE model of the SHPB was based on the actual device (Fig. 2). It consists of gas gun, striker (d=20 mm, L=150 mm), copper pulse and shaper (both: d=5 mm, H=3 mm), incident bar and transmission bar (both: d=20 mm, L=2000 mm).

Numerical analyses were performed using explicit LS-Dyna solver with central difference scheme and with the implementation of modified equation of motion time integration (Klepaczko, 2007). In the carried out analyses the stability of computations was guaranteed by Courant-Friedrichs-Lewy (CFL) condition, which can be described as follows [14]:

$$C = \frac{u_x \Delta t}{\Delta x} + \frac{u_y \Delta t}{\Delta y} + \frac{u_z \Delta t}{\Delta z} \le C_{\max} \tag{6}$$

where: u_x, u_y, u_z – velocities, Δt – time step, Δx, Δy, Δz – length intervals, C_{max} – varies with the method used (in presented investigations it was set to C_{max}=0.66, which is recommended for strongly dynamic phenomena).

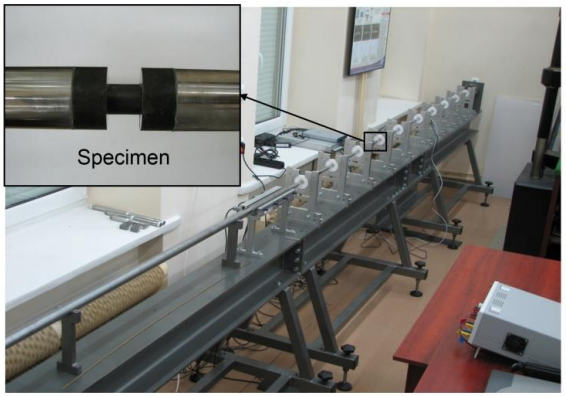

Fig. 2. Split Hopkinson Pressure Bar device used for the FE model

With the usage of finite element method the numerical model of SHPB apparatus was developed and validated (Baranowski et al., 2013). From the carried out simulations the incident impulse (axial stress) was obtained which was taken from the incident bar element from the same place, where strain gauge was glued. This choice of this particular element was dictated by the fact, that there were no differences between the stress values of the elements along the cross section area, whereas at the impact side of the bar these differences were noticed (Saint-Venant's principle was fully confirmed (Saint-Venant, 1855)). By comparing both pulses (experimental and numerical) good overall correlation was noticed: time intervals between incident and reflected impulses as well as stress values were approximately identical (Fig. 3)

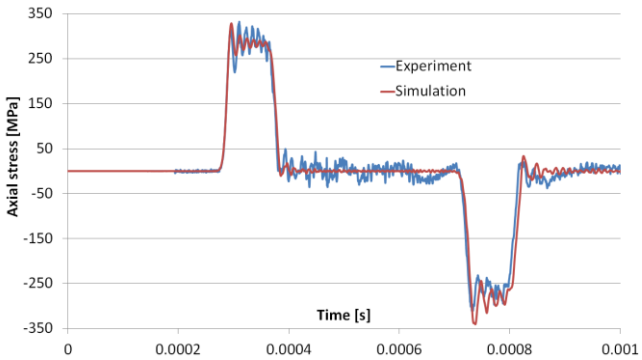

Fig. 3. Numerical and experimental impulse comparison in SHPB validation

In order to simplify and shorten computational time, symmetry of the problem was assumed and only quarter of the 3D model was taken into consideration. It is known that axially-symmetric model is less computationally expensive but chosen three-dimensional model in subsequent investigations will give the possibility to study additional effects, like dispersion effects or misalignment impacts occurring in the SHPB.

As mentioned before, copper sample was modelled using FE

VERSITA
DOI 10.2478/ama-2013-0033

and SPH mesh and for analyses with shaped incident pulse, the copper disc was described only using Lagrangian elements (Figs. 4-7). Also, dimensions of the sample were the same as in the pulse shaper (5 mm diameter, 3 mm long).

Initial velocity conditions were applied on the whole striker volume (all nodes), which values were as follows:

- v_1= 30 m/s,
- v_2= 25 m/s,
- v_3= 20 m/s.

At this point it should be also mentioned that proper contact definition is extremely important in numerical modelling of such strong dynamic phenomenon. More particular, it directly influences obtained incident impulse shape, which in fact, have an impact on the behaviour of a material sample. Thus, for the purpose of simulations surface to surface and nodes to surface contact algorithm with soft constraint option was applied, which guaranteed penetration not to occur (Hallquist, 2003). Generally, LS-DYNA, apart from the other, uses so called penalty function (Hallquist, 2003; Vulovic et al., 2007; Baranowski et al., 2012). Then, a fictional elastic element stiffness is added to the basic dynamic FE equilibrium thanks to the following energetic part:

$$\pi(u) = \kappa[(\mathrm{B}u - g_N)^T(\mathrm{B}u - g_N)] \tag{7}$$

where: u – global displacement vector, κ – fictional elastic element stiffness, B – matrix of boundary conditions kinematic, g_N – initial vector between the node and segment in contact.

Material properties for the bars were described with a typical Hooke's law elastic constitutive model (with literature steel data) since the incident and striker bar remain elastic during tests (Ellwood et al., 1982).

It is well known that the maximum stresses rises with strain rates, which also influence yielding of a material (Chmielewski at al., 2004; Janiszewski, 2012) and in presented studies copper sample, as well as the shaper, deforms in dynamic conditions where strain rate plays significant role (in the material the viscous effects are initiated). Thus, in both cases of sample modelling (FE and SPH) the Johnson-Cook constitutive material model was utilized (Tab. 1). It provides a prediction of flow stress σ_{flow} for arge strains and high strain rates, where its dependence on strain rate is linear in semi logarithmic scale (Hallquist, 2003; Johnson and Cook, 1983):

$$\sigma_{flow} = \left[A + B\left(\varepsilon^p\right)^n\right]\left(1 + C\ln\dot{\varepsilon}_*^p\right) \tag{8}$$

where A, B, C, n – material constants, ε^p – effective plastic strain, $\dot{\varepsilon}_*^p$ – effective plastic strain rate.

The Grüneisen equation of state was used for describing the pressure-volume relationship of the copper sample and pulse shaper with constants taken from literature (Steinberg, 1906) (Tab. 2). It defines the pressure in compressed materials as (Hallquist, 2003):

$$p = \frac{\rho_0 C^2 \mu\left[1 + \left(1 - \frac{\gamma_0}{2}\right)\mu - \frac{a}{2}\mu^2\right]}{\left[1 - (S_1 - 1)\mu - S_2\frac{\mu^2}{\mu+1} - S_3\frac{\mu^3}{(\mu+1)^2}\right]^2} + (\gamma_0 + a\mu)E \tag{9}$$

and for expanded materials as (Hallquist, 2003):

$$p = \rho_0 C^2 \mu + (\gamma_0 + a\mu)E \tag{10}$$

where C – intercept of the v_s-v_p curve (shock wave velocity vs. particle velocity), S_1,S_2,S_3 – coefficients of the slope of v_s-v_p curve, γ_0 – Grüneisen gamma, a – first order volume correction to γ_0, and $\mu = \rho/\rho_0 - 1$.

Tab. 1. Properties of copper for J-C model adopted in analyses [20]

A [MPa]	B [MPa]	N	C	ρ [kg/m3]	E [GPa]	υ
92	292	0.310	0.025	1.09	115	0.33

Tab. 2. Constants required for input in the Grüneisen EOS [21]

C_0 [m/s]	S_1	S_2	S_3	γ_0
3933	1.5	0	0	1.99

3.1. FE copper sample modelling

In the FE modelling of copper sample fully integrated hexagonal elements were used (HEX8). Also, symmetry conditions were applied and only quarter of the 3D model was taken into consideration. Two analyses were carried out: with and without the copper shaper (Fig. 4 and Fig. 5). For modelling the sample as well as pulse shaper large aspect ratio elements were chosen which guaranteed the accuracy and stability of computations throughout analysis in which the copper becomes largely compressed.

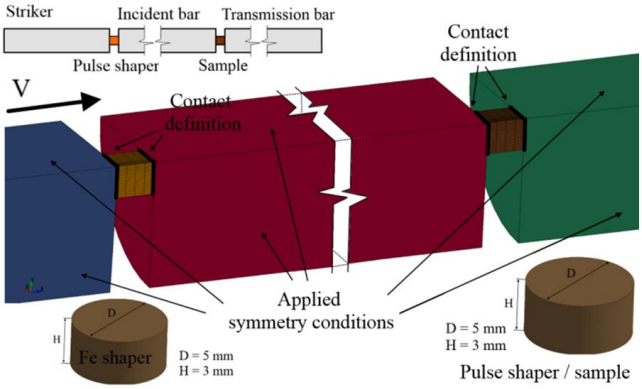

Fig. 4. Initial-boundary conditions applied for FE analysis with shaper

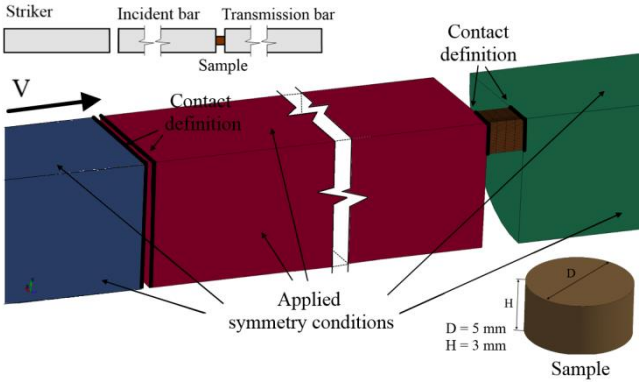

Fig. 5. Initial-boundary conditions applied for FE analysis without shaper

Interaction between striker, bars, copper disc and sample was described by the surface to surface contact procedure and no friction was assumed, which in actual conditions is reduced

as much as possible by adding a lubricate. As stated before three velocities were used, which resulted in different strain rates during tests.

3.2. SPH copper sample modelling

Smoothed Particles Hydrodynamics is a mesh-free particle method with Lagrangian nature, where computational information including mass and velocity are carried with particles. This method is mainly used for simulating fluid flows and large deformations of structures. The main difference between classical methods and SPH is the absence of a grid. Therefore, those particles are the framework of the region within the governing equations are solved (Hallquist, 2003). SPH method uses the concept of kernel and particle approximation as follows (Hallquist, 2003):

$$\Pi^k f(x) = \int f(y) W(x-y,h) dy \tag{11}$$

where W – kernel function, which is defined using the function θ by the relation:

$$W(x,h) = \frac{1}{h(x)^d} \theta(x) \tag{12}$$

where d is the number of space dimensions and h is the so-called smoothing length which varies in time and in space.

SPH model of the sample (with the same dimensions as previous) consisted of 468 elements with the average distance between particles 0.035 mm (Fig. 6, 7). It should be noted that authors used a "cylinder" method for the sample modelling. This choice was dictated by the fact, that is such strong-dynamic phenomena one of the main conditions for proper analysis is that the SPH mesh must be as regular as possible and must not contain too large variations (Hallquist, 2003).

In this case the interaction between SPH sample and bars was described by the nodes to surface contact procedure. Also, no friction was assumed and quarter of the model was applied. Additionally, recommended values of bulk viscosity for SPH formulation were used in presented investigations, i.e. Q1 = 1.5 and Q2 = 1.0.

Identical to the FE case three velocities were used and two analyses were carried out: with and without the copper shaper (Fig. 6 and Fig. 7).

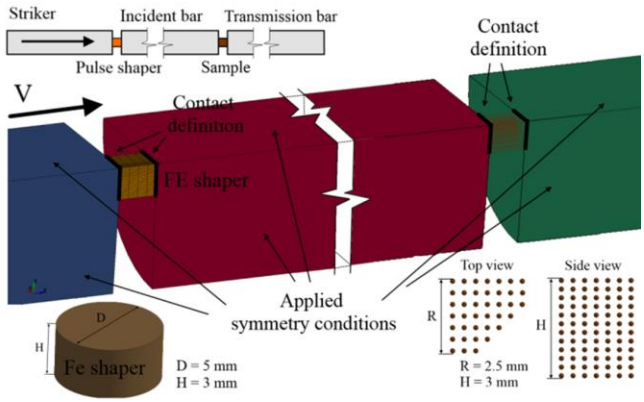

Fig. 6. Initial-boundary conditions applied for SPH analysis with shaper

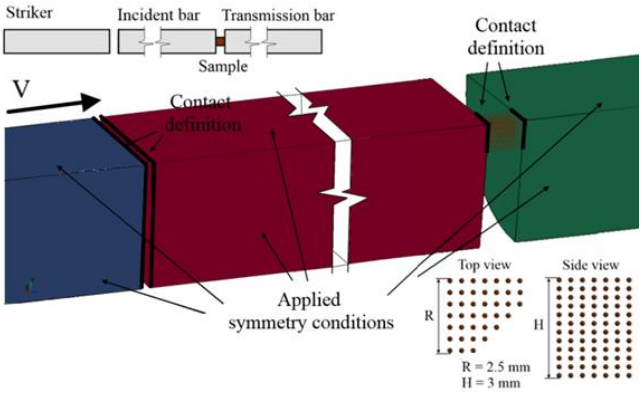

Fig. 7. Initial-boundary conditions for SPH analysis without shaper

4. RESULTS

From the performed simulations axial stress versus axial strain characteristics were obtained for all cases. In order to create curves an average value of all elements modelling specimen was taken into consideration. In Fig. 9, 12 copper sample stress-strain characteristic is presented for analyses (FE and SPH) with the shaper for three aforementioned different velocities. In Fig. 10, 13 the same result is presented but without impulse shaping, also for FE and SPH analysis.

For the FE analyses with shaper maximum axial stress achieved for v_1= 30 m/s, v_2= 25 m/s and v_3= 20 m/s were approximately 430 MPa, 406 MPa and 374 MPa, respectively. In the similar analysis (FE sample) but without shaper these values were as follows: 447 MPa, 418 MPa and 393 MPa. Also, one can see that by using the pulse shaper the incident pulse, which directly affects the material behaviour during compression, changes: its rise time increases and no oscillations can be noticed (Naghdabadia et al., 2012; Baranowski et al., 2013) (Fig. 8). On the other hand the decrease of the maximum axial stress in the specimen is clearly visible. Bearing this in mind and the fact that other authors obtained similar results (Naghdabadia et al., 2012; Janiszewski, 2012; Sankaye, 2011; Wu and Gorham, 1997) our curves can be regarded as appropriate and reasonable.

In the SPH analyses, also, similar results were obtained as in the FE case. Inserting the copper pulse shaper caused that the specimen deformation was reduced, which resulted in decrease of maximum axial stress and axial strain. Maximum axial stress obtained for those analyses were: 400 MPa, 384 MPa, 357 MPa with shaper and 410 MPa, 397 MPa and 376 MPa without the shaper. Figs. 11, 14 show the comparison graphs for each method.

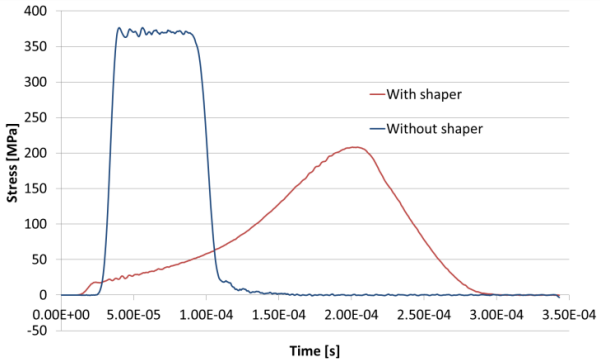

Fig. 8. Exampary incident pulse obtained in the simulation with and without shaper

DOI 10.2478/ama-2013-0033

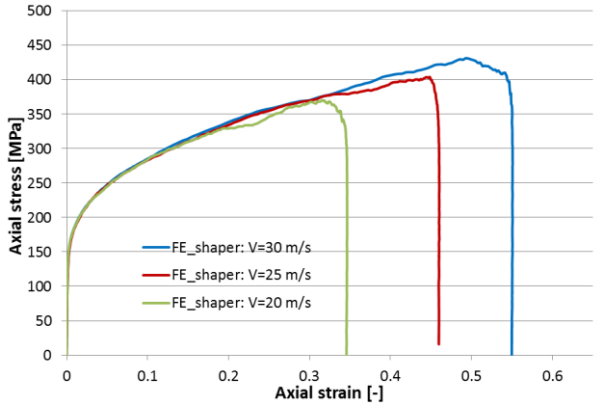

Fig. 9. Stress-strain characteristic for the FE modelling with shaper

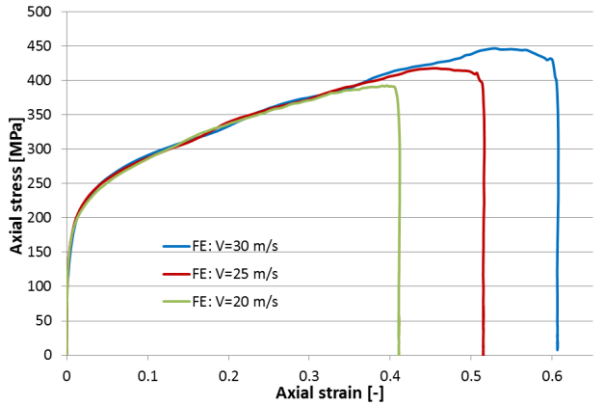

Fig. 10. Stress-strain characteristic for the FE modelling without shaper

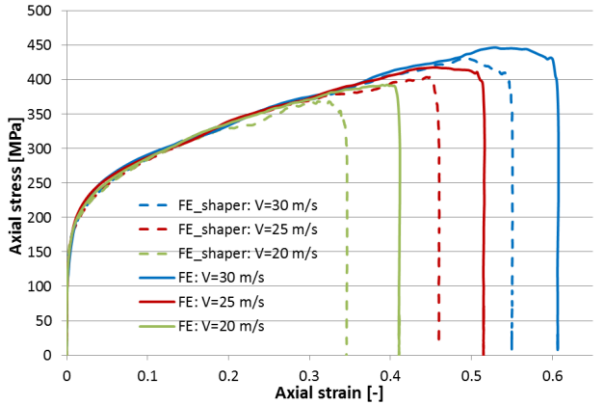

Fig. 11. Stress-strain characteristics comparison for the FE modelling

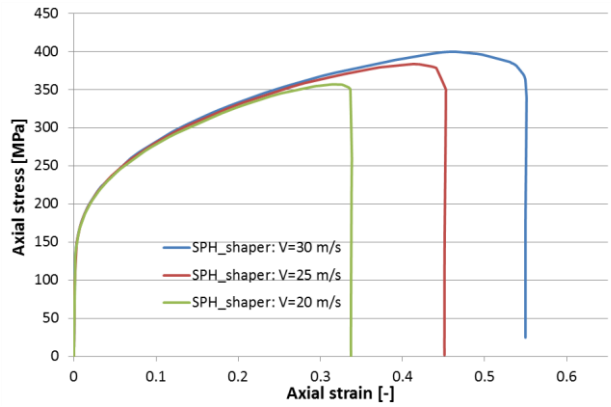

Fig. 12. Stress-strain characteristic for the SPH modelling with shaper

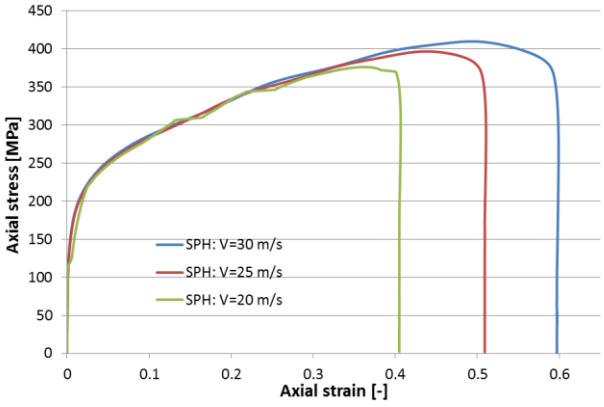

Fig. 13. Stress-strain characteristic for the SPH modelling without shaper

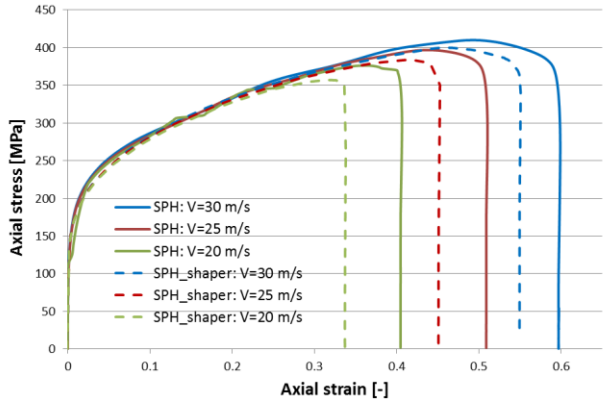

Fig. 14. Stress-strain characteristics comparison for the SPH modelling

4.1. FE and SPH method comparison

Figs. 15, 16 present both methods stress-strain curves for the same initial-boundary conditions. It is clearly seen that the stress and strain values obtained in SPH analyses are smaller than in FE modelling. It is caused by the fact that each element formulation handles deformation, and consequently, stresses in different way (Hallquist, 2003; Li and Liu, 2002). Differences (max stress values) between those two methods are listed in Tab.3.

It is worth to mention about the effectiveness of implemented methods (for the same termination time t_{end} = *0.0009 s* and for the same striker's velocity *v=30 m/s*). SPH formulation, due to the complex mathematical background, is much more computationally expensive – analyses were carried out for 104 min (without shaper) and 121 min (with shaper). In fact, it was also caused by the lower value of timestep, which is basically depended on the distances between particles (it was calculated as $dt = 2.80e^{-9}$). For the Lagrangian modelling the simulation (v=30 m/s) without shaper ended after 57 min, whereas with shaper after 73 min. In both cases timestep varied due to the large elements deformation as well as contact calculation: the approximate value equalled to $dt = 9.72e^{-9}$. The comparison graph is presented in Fig. 17. Also, as mentioned before, in order to perform simulations using SPH technique one of the main conditions for proper analysis is that the SPH mesh must be as regular as possible and must not contain too large variations. This indicated that there is a need to spend more time on developing a desired model.

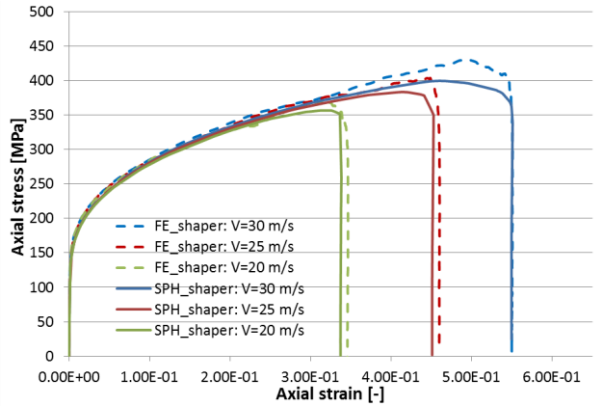

Fig. 15. Stress-strain characteristics comparison for FE and SPH modelling (shaper)

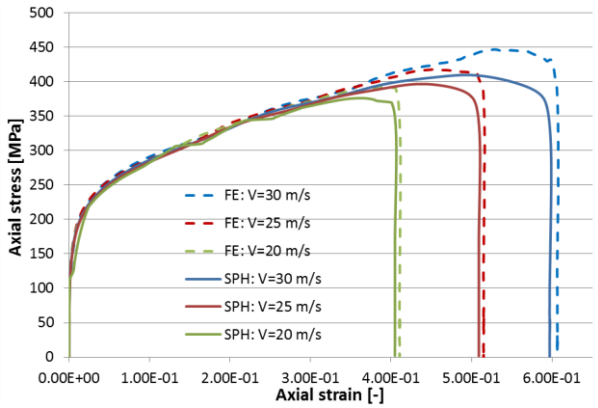

Fig. 16. Stress-strain characteristics comparison for FE and SPH modelling (no shaper)

Tab. 3. Statistic data (axial maximum stress) of obtained results

	Max. axial stress [MPa]			
	FE modelling		SPH modelling	
Impact velocity	Shaper	No shaper	Shaper	No shaper
30 m/s	430	447	400	410
25 m/s	406	418	383	397
20 m/s	374	393	357	376

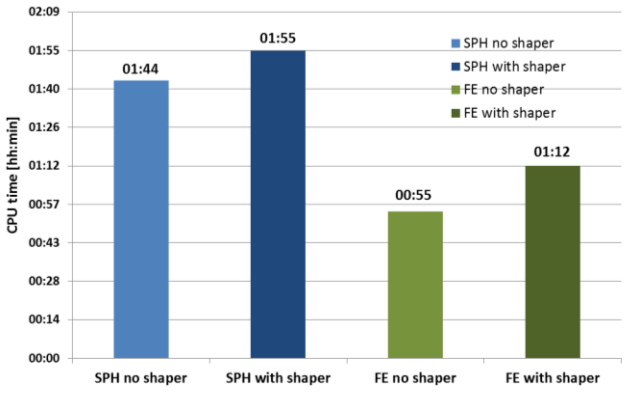

Fig. 17. CPU time comparison for all cases

5. CONCLUSIONS

The paper shows the possibility of two different numerical techniques for characterising a mechanical behaviour of material with and without copper disc between the striker and incident bar. For this purpose two available methods in LS-Dyna software were implemented to model the sample: typical finite element formulation (Lagrangian) and SPH – one of the most popular from meshless methods.

From the carried out analyses stress-strain histories for copper sample were obtained and examined. Simulations with and without the shaper were performed and two aforementioned methods were taken into consideration. The influence of copper disc on obtained results was investigated as well as both methods were compared with each other. It was proved that stress-strain characteristics shapes for both techniques are similar to those presented in available literature (Naghdabadia et al., 2012; Janiszewski, 2012; Sankaye, 2011; Wu and Gorham, 1997). Although, it seems that SPH modelling gives underestimated stress values and this needs to be verified in subsequent analyses with experimental validation. Moreover, SPH formulation, due to the complex mathematical background, is much more computationally expensive. Also it seems that for such short-lasting simulations of SHPB, time needed to prepare model is disproportionate. Nevertheless, in FE modelling of copper sample as well as shaper a special care must be taken to choose a proper aspect ratio of elements (min 4). In addition to being largely compressed they also maintain in contact with the bars so the accuracy of contact definition as well as stability of computations needs to be satisfied. Thus, both methods in terms of SHPB numerical testing have some disadvantages, but all in all the FE modelling seems to be more suitable for such phenomena. But one can see that some oscillations in stress-strain curves occur in FE modelling. Authors think that the main cause of such phenomena is the contact procedure, which is different from that used in SPH modelling and where slightly penetration was possible to occur. Also, in the free particle technique the artificial viscosity was used, which could also influenced the results.

Authors are aware that obtained stress-strain impulses would not provide constant strain rates during the tests (Naghdabadia et al., 2012; Wu and Gorham, 1997). Also, only one copper shaper was used whereas it is known that for different striker velocities and material (brittle, plastic etc.) various discs should be used: with large diameter and small length or vice versa (Naghdabadia et al., 2012). Nevertheless, for this part of investigations, which has the initial character, such results will be the basis for further testing including different diameter-length ratio studies. Moreover, as discussed in the previous authors' paper (Baranowski et al., 2013), main attention of authors' tests (with this paper as a part of them) is to find an ideal incident shape for the specific type of material using a special shaped striker or the copper shaper presented here. It is also worth to add that at present authors are performing experimental testing for validation of computational analyses and for obtaining the JC material properties of various materials. Taking into account the fact that both methods of modelling are verified the results obtained in future will be much more reliable, interesting and helpful in subsequent investigations.

DOI 10.2478/ama-2013-0033

REFERENCES

1. **Baranowski P., Bukała J., Damaziak K., Małachowski J., Mazurkiewicz L., Niezgoda T.** (2012), Numerical description of dynamic collaboration between rigid flying object and net structure, *Journal of Transdisciplinary Systems Science*, Vol. 16, No. 1, 79-89.
2. **Baranowski P., Malachowski J., Gieleta R., Damaziak K., Mazurkiewicz L., Kolodziejczyk D.** (2013), Numerical study for determination of pulse shaping design variables in SHPB apparatus (in print), *Bulletin of the Polish Academy of Sciences: Technical Sciences.*
3. **Chmielewski R., Kruszka L., Młodożeniec W.** (2004), The study of static and dynamic properties of 18G2 steel (in polish), *Biuletyn WAT*, Vol. 53, 31-45 .
4. **Cloete T.J., V.d. Westhuizen A., Kok S., Nurick G.N.** (2009), A tapered striker pulse shaping technique for uniform strain rate dynamic compression of bovine bone, *EDP Sciences*, 901-907.
5. **Davies R.M.** (1948), A critical study of the Hopkinson pressure bar, *Philosophical Transactions of the Royal Society of London*, Vol. 240, 375-457.
6. **Ellwood S., Griffiths L.J., Parry D.J.** (1982), Materials testing at high constant strain rates, *Journal of Physics E: Scientific Instruments*, Vol. 15, 280-282.
7. **Foley J.R., Dodson J.C., McKinion C.M.** (2010), *Split Hopkinson Bar Experiments of Preloaded Interfaces,* Proc. of the IMPLAST 2010 Conference.
8. **Franz C.E., Follansbee P.S., Berman I., Schroeder J.W.** (1984), *High energy rate fabrication*, American Society of Mechanical Engineers.
9. **Graff K.F.** (2004), *Wave Motion in Elastic Solids*, Dover Publications, New York.
10. **Hallquist J.O. (2003),** *LS-Dyna:Theoretical manual***,** California Livermore Software Technology Corporation.
11. **Hopkinson J.** (1872), On the rupture of iron wire by a blow, *Proc. Literary and Philosophical Society of Manchester*, 40-45.
12. **Janiszewski J.** (2012), *The study of engineering materials under dynamic loading* (in polish), Military University of Technology, Warsaw.
13. **Jankowiak T., Rusinek A., Lodygowski T.** (2011), Validation of the Klepaczko–Malinowski model for friction correction and recommendations on Split Hopkinson Pressure Bar, *Finite Elements in Analysis and Design*, Vol. 47, 1191-1208.
14. **Johnson G.R., Cook W.H.** (1983), *A constitutive model and data for metals subjected to large strains, high strain rated and high temperatures*, Proc. from the 7th International Symposium on Ballistics.
15. **Klepaczko J.R.** (2007), *Introduction to Experimental Techniques for Materials Testing at High Strain Rates*, Institute of Aviation, Scientific Publications Group.
16. **Li S., Liu W.K.** (2002), Meshfree and particle methods and applications, *Applied Mechanics Reviews,* Vol. 55. No. 1, 1-34.
17. **Li X.B., Lok T.S., Zhao J.** (2005), Dynamic Characteristics of Granite Subjected to Intermediate Loading Rate*, Rock Mechanics and Rock Engineering*, Vol. 38, No. 1, 21-39.
18. **Naghdabadia R., Ashrafia M.J., Arghavani J.** (2012), Experimental and numerical investigation of pulse-shaped split Hopkinson pressure bar test, *Materials Science and Engineering A*, Vol. 539, 285-293.
19. **Saint-Venant A. J. C. B**. (1855), Memoire sur la Torsion des Prismes, Mem. Divers Savants, Vol. 14, pp. 233–560.
20. **Sankaye S.S.** (2011), *Dynamic testing to determine some mechanical properties of aluminium, copper and dry eglin sand using Split Hopkinson Pressure Bar (SHPB), high speed phtography and digital image correlation (DIC),* Master of science thesis, Aurangabad, Maharashtra, India.
21. **Seng L.K.** (2003), Design of a New Impact Striker Bar for Material Tests in a Split Hopkinson Pressure Bar, *Civil engineering Research Bulletin*, Vol. 16, 70-71.
22. **Steinberg D.** (1906), *Equation of State and Strength Properties of Selected Materials*, Lawrence Livermore National Laboratory, Livermore, CA.
23. **Vulovic S., Zivkovic M., Grujovic N., Slavkovic R.A.** (2007), Comparative study of contact problems solution based on the penalty and Lagrange multiplier approaches, *J. Serbian Society for Computational Mechanics*, Vol. 1, No. 1, 174-183.
24. **Wu X.J., Gorham D.A.** (1997), Stress equilibrium in the Split Hopkinson Pressure Bar Test, *Journal of Physics IV France 7,* Vol. 3, 91-96.